Received: 21 May 2019 | Revised: 26 July 2019 | Accepted: 16 August 2019

DOI: 10.1111/all.14036

ORIGINAL ARTICLE

Allergen-Specific Immunotherapy and Biologics

Allergy EUROPEAN JOURNAL OF ALLERGY AND CLINICAL IMMUNOLOGY EAACI WILEY

Alum impairs tolerogenic properties induced by allergoid-mannan conjugates inhibiting mTOR and metabolic reprogramming in human DCs

Cristina Benito-Villalvilla[1] | Irene Soria[2] | Mario Pérez-Diego[1] | Enrique Fernández-Caldas[2,3] | José Luis Subiza[2] | Oscar Palomares[1]

[1]Department of Biochemistry and Molecular Biology, School of Chemistry, Complutense University, Madrid, Spain

[2]Inmunotek, Alcalá de Henares, Madrid, Spain

[3]University of South Florida, College of Medicine, Tampa, FL, USA

Correspondence
Oscar Palomares, Department of Biochemistry and Molecular Biology, School of Chemistry, Complutense University of Madrid, Avenida Complutense s/n, 28040 Madrid, Spain.
Email: oscar.palomares@quim.ucm.es

Funding information
Ministerio de Economía y Competitividad, Grant/Award Number: SAF-2017-84978-R; Centre for Industrial Technological Development, Grant/Award Number: IDI-20110410 and IDI-20141131

Abstract

Background: Polymerized allergoids conjugated to mannan (PM) are suitable vaccines for allergen-specific immunotherapy (AIT). Alum remains the most widely used adjuvant in AIT, but its way of action is not completely elucidated. The better understanding of the mechanisms underlying alum adjuvanticity could help to improve AIT vaccine formulations.

Objective: We sought to investigate the potential influence of alum in the tolerogenic properties imprinted by PM at the molecular level.

Methods: Flow cytometry, ELISAs, cocultures, intracellular staining and suppression assays were performed to assess alum and PM effects in human dendritic cells (DCs). BALB/c mice were immunized with PM alone or adsorbed to alum. Allergen-specific antibodies, splenocyte cytokine production and splenic forkhead box P3 (FOXP3)$^+$ regulatory T (Treg) cells were quantified. Metabolic and immune pathways were also studied in human DCs.

Results: Alum decreases PD-L1 expression and IL-10 production induced by PM in human DCs and increases pro-inflammatory cytokine production. Alum impairs PM-induced functional FOXP3$^+$ Treg cells and promotes Th1/Th2/Th17 responses. Subcutaneous immunization of mice with PM plus alum inhibits in vivo induction of Treg cells promoted by PM without altering the capacity to induce functional allergen-specific blocking antibodies. Alum inhibits mTOR activation and alters metabolic reprogramming by shifting glycolytic pathways and inhibiting reactive oxygen species (ROS) production in PM-activated DCs, impairing their capacity to generate functional Treg cells.

Conclusion: We uncover novel mechanisms by which alum impairs the tolerogenic properties induced by PM, which might well contribute to improve the formulation of novel vaccines for AIT.

Abbreviations: 2-DG, 2-deoxy-D-glucose; AIT, allergen-specific immunotherapy; Alum, aluminium hydroxide; Breg, regulatory B; CLRs, C-type lectin receptors; DCs, dendritic cells; FOXP3, forkhead box P3; HmoDC, human monocyte-derived dendritic cell; mDC, myeloid dendritic cell; mTOR, mammalian target of rapamycin; N, native grass pollen extract; NAC, N-acetyl-L-Cysteine; OX40L, OX40 ligand; pDC, plasmacytoid dendritic cell; PD-L1, programmed death-ligand 1; PM, polymerized allergoids conjugated to mannan; PTEN, phosphatase and tensin homologue; ROS, reactive oxygen species; Treg, regulatory T; $\Delta\psi$, membrane potential.

This is an open access article under the terms of the Creative Commons Attribution-NonCommercial License, which permits use, distribution and reproduction in any medium, provided the original work is properly cited and is not used for commercial purposes.
© 2019 The Authors. *Allergy* published by John Wiley & Sons Ltd.

KEYWORDS
allergen-specific immunotherapy, alum, dendritic cells, polymerized allergoids conjugated to mannan, regulatory T cells

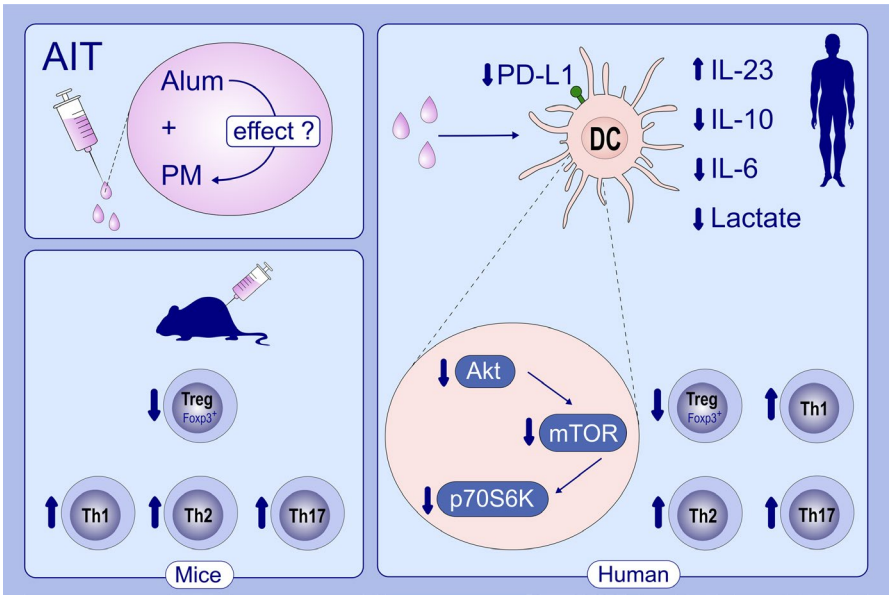

GRAPHICAL ABSTRACT

This study investigated the potential influence of alum in the tolerogenic properties imprinted by PM. Alum decreased expression of PD-L1 and production of IL-10, IL-6 and lactate, increased IL-23 release and inhibited mTOR activation in PM-activated DCs. Alum suppressed PM-induced functional FOXP3$^+$ Treg cells and promoted Th1/Th2/Th17 responses.

Abbreviations: Akt, protein kinase B; Alum, aluminium hydroxide; FOXP3, forkhead box P3; mTOR, mammalian target of rapamycin; P70S6K, 70 kDa ribosomal protein S6 kinase; PD-L1, programmed death ligand 1; PM, polymerized-allergoids conjugated to mannan; ROS, reactive oxygen species

1 | INTRODUCTION

Allergen-specific immunotherapy (AIT) is the only treatment with potential long-lasting disease-modifying effects for allergic diseases.[1-3] Successful AIT is associated with a very rapid desensitization of mast cells and basophils and with the inhibition of type 2 immune-mediated responses. Sustained tolerance after AIT discontinuation requires the generation and preservation of functional allergen-specific regulatory T (Treg) and B (Breg) cells as well as allergen-specific blocking antibodies.[4-6] Clinical trials and real-life practice demonstrated AIT as an effective treatment; however, it still faces several drawbacks regarding the long treatment duration, patient compliance, side effects or low efficacy for some patients.[3,7,8] Polymerized allergoids conjugated to mannan (PM) have been recently reported as next-generation vaccines targeting dendritic cells (DCs) that might well contribute to overcome such inconveniences.[9-12] PM are captured very efficiently by human DCs via mannose receptor and other C-type lectin receptors (CLRs). PM activates CLRs and promotes IL-10-producing tolerogenic DCs that generate functional forkhead box P3 (FOXP3)$^+$ Treg cells through programmed death-ligand 1 (PD-L1).[9,10] In mice, subcutaneous or sublingual immunization with PM increases the frequency of splenic FOXP3$^+$ Treg cells and induces healthy immune responses to allergens.[9,11,13] All these beneficial effects depend on the structural integrity of the conjugated mannan.[9,12-14]

Aluminium hydroxide (alum) remains the most widely used adjuvant in AIT.[15-17] For long time, the main effects attributed to alum have been related to its depot effect leading to the slow release of the adsorbed allergens.[15,18] Alum also activates innate immune responses in DCs and macrophages. Alum induces the release of uric acid and double-stranded DNA, which activate NLRP3 inflammasome and IRF3 leading to the production of pro-inflammatory cytokines.[19,20] In addition, alum activates Syk-PI3kδ pathways and induces PGE2 production, which is involved in Th2 polarization.[19,20] However, the detailed molecular mechanisms driving alum adjuvanticity still remain largely unknown.[15,18]

Metabolic reprogramming in immune cells refers to the changes occurring after activation in the intracellular metabolic pathways that lead to functional regulation.[21] DCs' function is finely regulated by metabolic reprogramming in cooperation with immune pathways.[22] The change in metabolism towards glycolysis with high lactate production despite the availability of oxygen is known as the Warburg effect, which represents a key event in the

regulation of DCs' function.[21,22] Mammalian target of rapamycin (mTOR) is an important regulator of metabolic reprogramming, and its activation state is highly responsive to intracellular and extracellular signals.[21,22] How DCs simultaneously activated with alum and CLR ligands drive immune responses and the potential consequences of this cross-talk in metabolic reprogramming remains fully elusive.

The better understanding of the mechanisms involved in alum adjuvanticity might well contribute to improve vaccine formulations for AIT. Herein, we show for the first time that alum impairs the tolerogenic features imprinted by allergoids conjugated to mannan in human DCs. Alum inhibits PM-induced functional FOXP3$^+$ Treg cells and promotes Th1/Th2/Th17 responses. In vivo, subcutaneous immunization of mice with PM adsorbed to alum inhibits the healthy immune responses to allergens induced by PM alone. Alum shifts glycolytic pathways, inhibits mTOR activation and impairs reactive oxygen species (ROS) production in PM-activated DCs, thus inhibiting their capacity to generate functional Treg cells. Collectively, we uncover novel mechanisms by which alum impairs the tolerogenic properties induced by PM, which might well pave the way not only for the future rational design of novel AIT vaccines but also for other vaccine formulations.

2 | METHODS

2.1 | Material, media and reagents

For cell cultures, we used RPMI 1640 (Lonza) supplemented with 10% heat-inactivated foetal bovine serum, 100 μg/mL normocin (InvivoGen), 50 μg/mL penicillin-streptomycin, 1% nonessential amino acids, 1% MEM vitamins and 1 mmol/L sodium pyruvate (Life Technologies). Glutaraldehyde-polymerized grass pollen (*Phleum pratense)* allergoids conjugated to nonoxidized mannan (PM) and native grass pollen *P pratense* allergens (N) were provided by Inmunotek SL. Aluminium hydroxide gel (Alhydrogel) was from InvivoGen. Inhibitors for mTOR (rapamycin) (InvivoGen), ROS (N-acetyl-cysteine (NAC)) or glycolysis (2-Deoxy-D-glucose (2-DG)) (Sigma-Aldrich) were used for the inhibition experiments.

2.2 | Cell cultures

Immature hmoDCs or human total blood DCs from healthy donors or allergic patients (10^6 cells per mL) were stimulated with medium (Ctrl -), alum (0.1 mg/mL), PM (50 μg/mL) or PM with alum for 18 hours. PM were adsorbed to alum with continuous stirring for 2 hours. Cell pellets were used to analyse their phenotype by flow cytometry and cell-free supernatants to quantify IL-6, IL-23, IL-12, IL-4 and IL-10 by ELISA. For inhibition experiments, hmoDCs were preincubated for 1 hour with 2-DG (10 mmo/L) or NAC (25 mmo/L), or for 30 minutes with rapamycin (100 nmo/L) (or corresponding vehicle controls) prior to activation. Then, the cells were stimulated with the stimulus for 18 hours in the presence of the corresponding inhibitors to quantify IL-10 by ELISA or PD-L1 by flow cytometry. Cell viability was analysed in all the cases by trypan blue exclusion with a light microscope.

2.3 | Statistical analysis

In all experiments, data represent the mean ± SEM of the indicated parameters. Statistical differences were determined with the paired or unpaired Student *t* test using Prism software 6.0 (GraphPad Software). Significance is indicated in each figure.

All procedures used in this study are fully described in the Methods section in this article's Data S1.

3 | RESULTS

3.1 | Alum impairs tolerogenic features imprinted by PM in human DCs

To analyse the impact of alum on the expression pattern of different surface molecules and cytokine production induced by PM in human DCs, we treated human monocyte-derived dendritic cells (hmoDCs) or an enriched fraction of total DCs with PM alone or with PM plus alum. The expression of the inhibitory molecule PD-L1 was significantly reduced in PM-stimulated hmoDCs in the presence of alum (Figure 1A). In contrast, alum significantly increased the expression of CD-83 and OX40 ligand (OX40-L), which are molecules associated with mature DCs and amplification of Th2 cell responses, respectively.[23,24] There were no significant differences in HLA-DR expression (Figure 1A). Representative histograms are displayed in Figure 1B. HmoDCs activated by PM in the presence of alum produced significantly higher levels of the pro-inflammatory cytokine IL-23 than PM-stimulated hmoDCs (Figure 1C). We did not detect IL-12 or significant differences in IL-4 production (Figure 1C). Alum significantly reduced the production of IL-6 and the anti-inflammatory cytokine IL-10 in PM-activated hmoDCs (Figure 1C). Remarkably, alum alone only induced significant production of IL-23 but not any of the other assayed cytokines. Next, we isolated an enriched fraction of human blood total DCs containing both plasmacytoid DCs (pDCs) and myeloid DCs (mDCs) (Figure 1D). Supporting our data in hmoDCs, alum significantly increases the production of IL-23 by PM-treated total blood DCs. IL-10 and IL-6 production also tends to decrease in the presence of alum in PM-activated total blood DCs (Figure 1E).

3.2 | Alum promotes Th1, Th2 and Th17 responses and decreases IL-10-producing T cells induction by PM-activated human DCs

To determine the capacity of human DCs stimulated with PM in the presence of alum to polarize CD4$^+$ T-cell responses, we performed coculture experiments. HmoDCs activated with PM plus alum generated T cells producing higher levels of IFN-γ, IL-5 and IL-17A than hmoDCs stimulated with PM alone (Figure 2A). In contrast, PM-activated hmoDCs in the presence of alum generated T cells producing

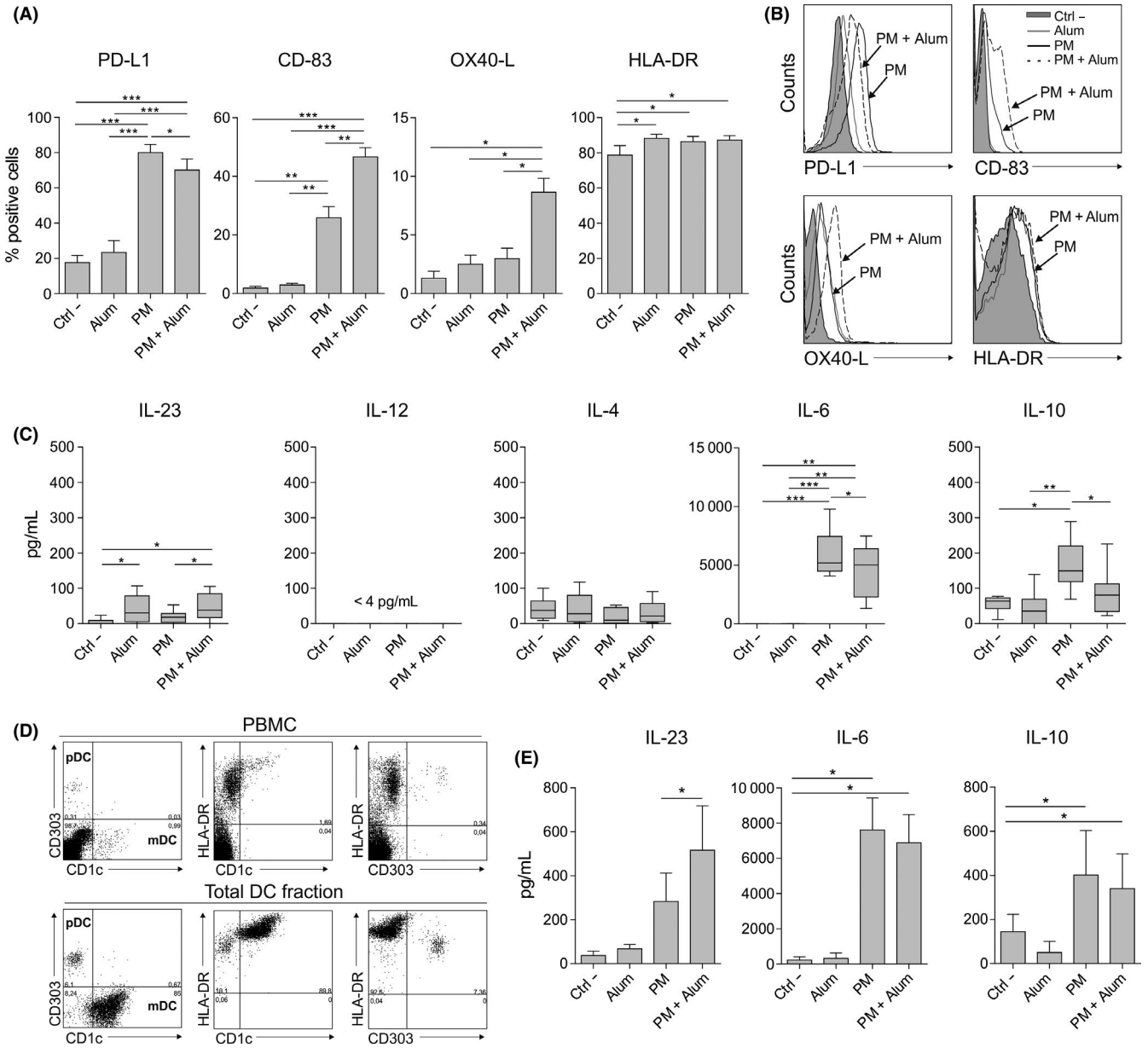

FIGURE 1 Alum alters the phenotype and function induced by PM in human DCs from healthy donors. A, Percentage of positive cells after stimulation of hmoDCs with medium (Ctrl -), alum, PM or PM with alum for 18 h (n = 5-7). B, Flow cytometry representative histograms. C, Cytokine production after stimulation of hmoDCs with the indicated stimulus for 18 h (n = 7). D, Representative dot plots for pDCs and mDCs in PBMCs and the enriched total DC fraction. E, Cytokine production after stimulation of total blood DCs with the indicated stimulus for 18 h (n = 6). Paired Student *t* test: **P* < .05, ***P* < .01 and ****P* < .001

less IL-10 than PM-activated hmoDCs (Figure 2A). The IFN-γ/IL-10, IL-5/IL-10 and IL-17A/IL-10 ratios were significantly higher when T cells were primed by hmoDCs activated with PM plus alum than with PM alone (Figure 2B). To verify these data at the single-cell level, we performed intracellular staining experiments. Primed $CD4^+$ T cells were restimulated with PMA/ionomycin in the presence of brefeldin A. Supporting our results, the percentages of IFN-γ-, IL-5- and IL-17A-producing $CD4^+$ T cells generated by hmoDCs activated with PM in the presence of alum were significantly higher than with PM alone. The percentage of IL-10-producing $CD4^+$ T cells was significantly decreased in the presence of alum (Figure 2C). Representative dot plots are displayed in Figure 2D. Coculture experiments using an enriched fraction of total blood DCs demonstrated that T cells primed by blood DCs activated with PM in the presence of alum produced higher amounts of IFN-γ, IL-5 and IL-17A and significantly lower levels of IL-10 than T cells generated by total DCs activated with PM alone (Figure 2E). The IFN-γ/IL-10, IL-5/IL-10 and IL-17A/IL-10 ratios were significantly increased in the presence of alum (Figure 2F). Similar results were obtained in longer cocultures performed during 10 days (data not shown).

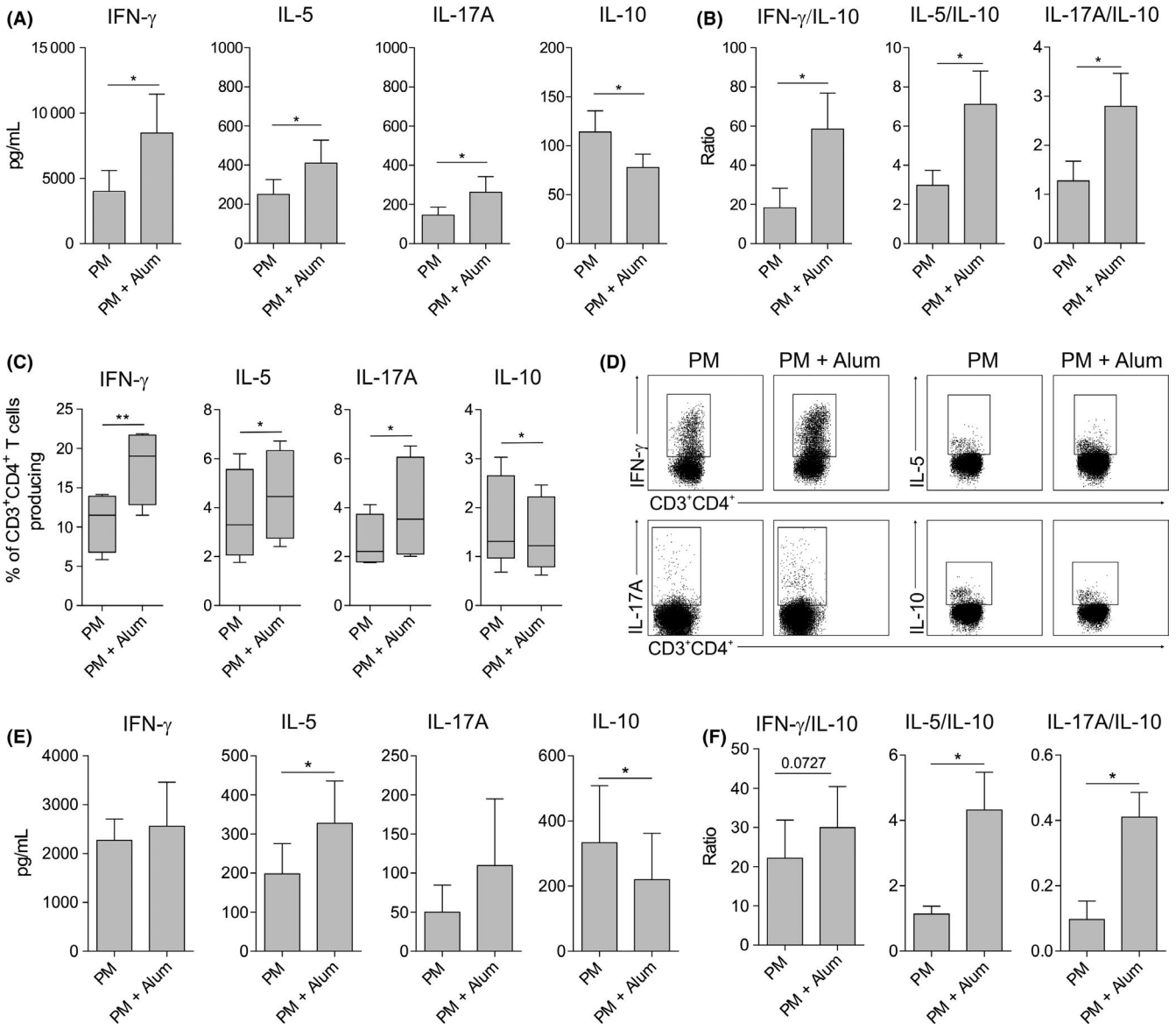

FIGURE 2 Alum promotes the generation of Th1, Th2 and Th17 cells and impairs the induction of IL-10-producing T cells by PM. A and B, Cytokines (A) or cytokine ratios (B) produced by allogeneic naïve $CD4^+$ T cells primed by PM- or PM and alum-activated hmoDCs from healthy donors after 5 d (n = 6). C, After 5 d of coculture, primed T cells were washed and stimulated for 6 h with PMA/ionomycin in the presence of brefeldin A. Percentage of $CD3^+CD4^+$ T cells producing the indicated cytokines after intracellular staining and flow cytometry analysis (n = 4). D, Representative dot plots for the intracellular staining after flow cytometry analysis. E and F, Cytokines (E) or cytokine ratios (F) produced by allogeneic naïve $CD4^+$ T cells primed by PM- or PM and alum-activated total blood DCs from healthy donors after 5 d (n = 5). Paired Student *t* test: *$P < .05$ and ** $P < .01$

3.3 | Alum impairs the generation of functional $FOXP3^+$ Treg cells by PM-activated DCs

PM-treated hmoDCs induced significantly higher numbers of $CD4^+CD25^{high}CD127^-FOXP3^+$ Treg cells than medium- or alum-treated hmoDCs. In the presence of alum, the number of $FOXP3^+$ Treg cells induced by PM-activated hmoDCs was significantly decreased (Figure 3A). For functional experiments, we sorted the generated Treg cells ($CD4^+CD25^{high}CD127^-$) (Figure S1A). Purified Treg cells generated by PM-activated hmoDCs suppressed autologous PBMCs in a dose-dependent manner (Figure S1B) and displayed a more potent suppression capacity than those generated in the presence of alum (Figure 3B). Purified non-Treg cells ($CD4^+CD25^-CD127^-$) from both conditions showed no suppression capacity (Figure 3B). Interestingly, PM-activated total DCs also generated a large number of $CD4^+CD25^{high}CD127^-FOXP3^+$ Treg cells, which was significantly reduced in the presence of alum, thus confirming the results obtained with hmoDCs (Figure 3C). We obtained the same results when hmoDCs from allergic patients were employed (Figure S2A). The cytokine signature of PBMCs from allergic patients and healthy donors

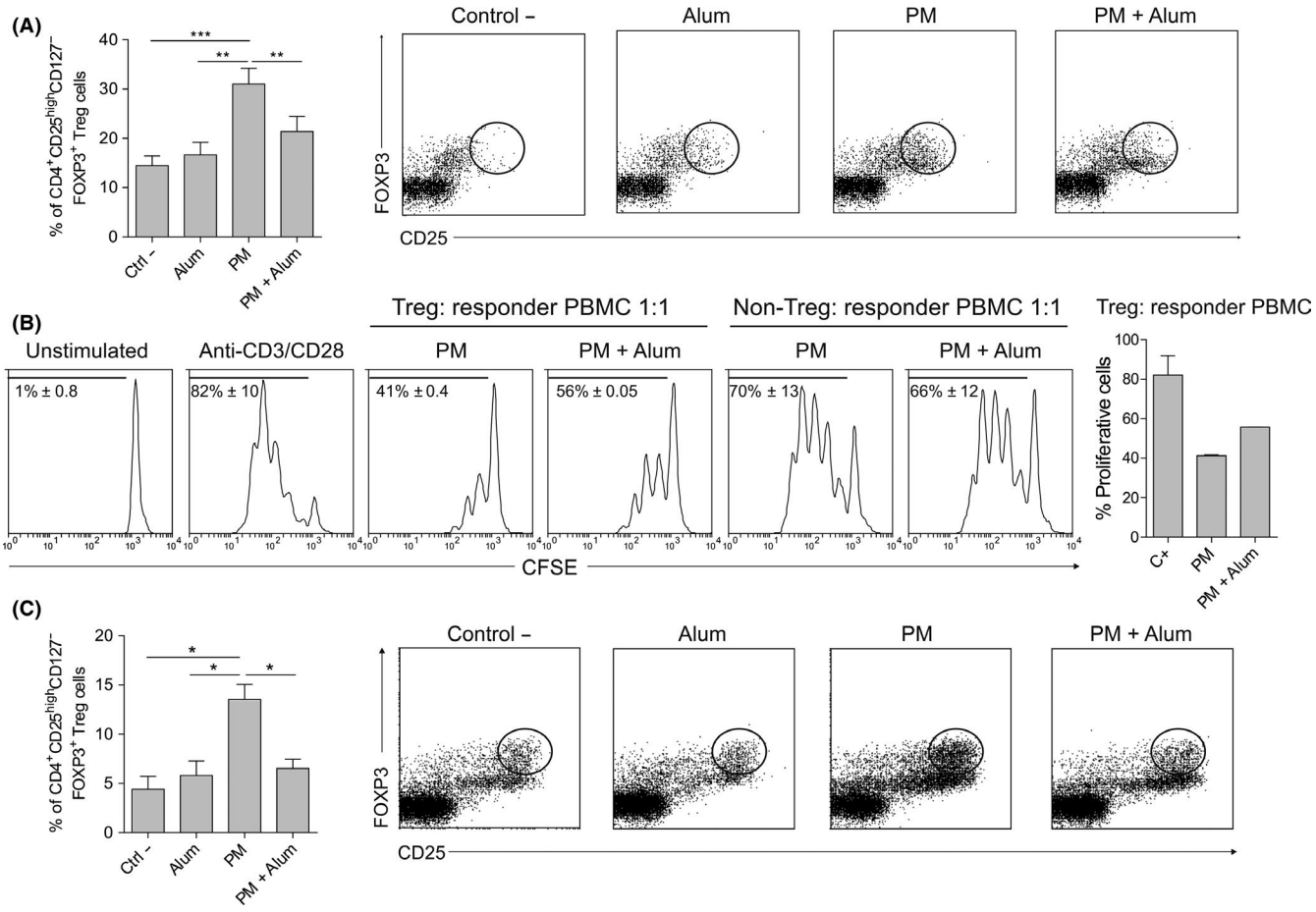

FIGURE 3 Alum reduces PM-induced functional FOXP3$^+$ Treg cells. A, Percentage of induced CD4$^+$CD25^{high}CD127$^-$FOXP3$^+$ Treg cells by allogeneic medium (Ctrl -)-, alum-, PM- or PM and alum-treated hmoDCs from healthy donors after 5 d (gating in lymphocytes, n = 9). B, Proliferation of CFSE-labelled PBMCs gated on CD4$^+$ T cells after 5 d of coculture with autologous purified FOXP3$^+$ Treg cells generated by allogeneic PM- or PM and alum-treated hmoDCs (ratio 1:1). The percentage of proliferating responder PBMCs stimulated with anti-CD3 and anti-CD28 for each condition at a 1:1 ratio is shown (n = 2). C, CD4$^+$CD25^{high}CD127$^-$FOXP3$^+$ Treg cells generated by allogeneic medium (Ctrl -)-, alum-, PM- or PM and alum-treated total blood DCs after 5 d (gating in lymphocytes, n = 4). Paired Student *t* test: **P* < .05, ***P* < .01 and ****P* < .001

stimulated with PM alone or with PM in the presence of alum was also comparable and characterized by reduced IL-10 production and increased INF-γ/IL-10 ratio in the presence of alum (Figure S2B,C). These results confirm our previous data showing that PM is able to induce similar responses in allergic patients and healthy donors.[9]

3.4 | Immunization of BALB/c mice with PM in the presence of alum impairs the healthy immune responses to allergens imprinted by PM

To assess the in vivo relevance of our findings, we immunized subcutaneously BALB/c mice with diluent (Ctrl -), alum, PM or PM plus alum, following the protocol showed in Figure 4A and analysed the indicated parameters. Splenocytes from mice immunized with PM plus alum produced significantly higher levels of IFN-γ, IL-5 and IL-4 but less IL-10 after in vitro stimulation with native grass pollen extract (N) than those from mice immunized with PM alone (Figure 4B). The ratios IL-10/IFN-γ and IL-10/IL-5 were significantly lower in the presence of alum (Figure 4C). Interestingly, the percentage of splenic FOXP3$^+$ Treg cells was significantly higher in mice immunized with PM than diluent (Ctrl -), which was significantly impaired in the presence of alum (Figure 4D). The levels of serum IgG1 and IgE antibodies specific for native grass pollen allergens were higher in mice immunized with PM plus alum than in mice immunized only with PM, whereas the levels of IgG2a were not significantly different between these two groups (Figure 4E). The IgG1/IgG2a ratio was significantly higher in mice immunized with PM plus alum than with PM alone (Figure 4F). Next, we assessed the capacity of the antibodies generated in mice after each immunization to block patients' IgE binding to native grass pollen extract. Although the antibodies induced with PM in the presence of alum display a slight higher blocking activity than those generated by PM alone, significant differences were not observed, indicating that alum does not significantly enhance the capacity of PM to generate allergen-specific blocking antibodies.

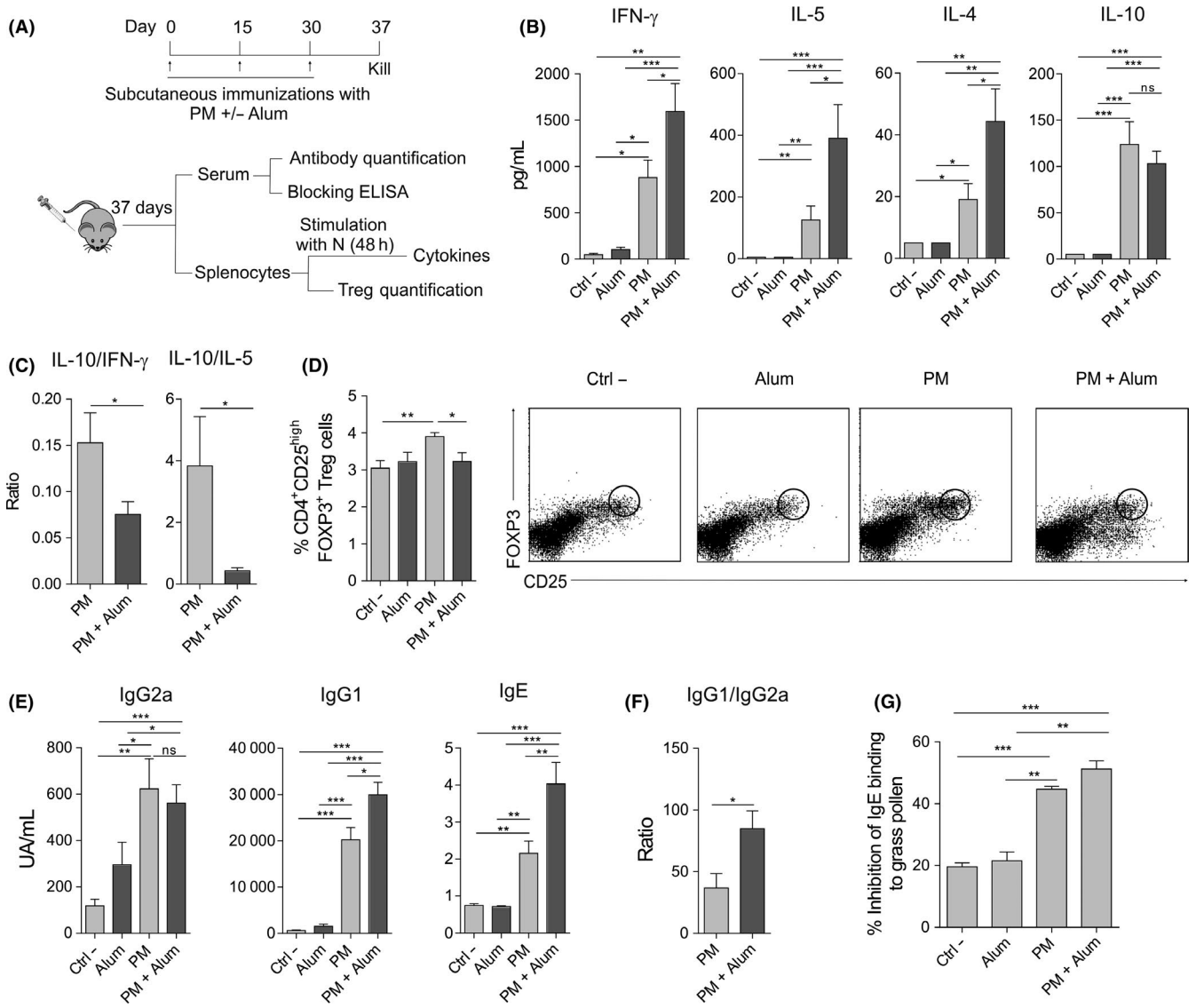

FIGURE 4 Alum impairs in vivo tolerogenic properties induced by PM in BALB/c mice. A, Scheme of the subcutaneous immunization protocol and analysis of induced systemic responses. B and C, Cytokine production (B) or cytokine ratios (C) by splenocytes from mice immunized subcutaneously with diluent (Ctrl -), alum, PM or PM and alum, and stimulated in vitro with native grass pollen extract. D, Percentage of $CD4^{+}CD25^{high}FOXP3^{+}$ Treg cells in spleens of mice immunized with diluent (Ctrl -), alum, PM or PM and alum. Representative dot plots are shown. E and F, Serum grass pollen-specific antibodies (E) or ratio of serum grass pollen-specific IgG1/IgG2a (F) from mice immunized with diluent (Ctrl -), alum, PM or PM and alum. G, Inhibition of serum IgE binding to native grass pollen allergens by blocking antibodies from mice immunized with diluent (Ctrl -), alum, PM or PM and alum (mean ± SEM of n = 5 grass pollen allergic patients). For panels B-F, values are mean ± SEM of 18 individual mice per condition of 3 independent experiments. Unpaired Student *t* test: **P* < .05, ***P* < .01 and ****P* < .001

3.5 | Alum alters metabolic reprogramming induced by PM and inhibits mTOR activation in human DCs

We studied changes in the metabolic state of DCs activated with PM and how this could be influenced by the presence of alum. HmoDCs activated with PM increased the production of lactate (Warburg effect) compared with unstimulated hmoDCs, which was significantly reduced when hmoDCs were stimulated with PM plus alum (Figure 5A,B). The stimulation of hmoDCs with PM significantly increased the consumption of glucose from the culture medium (Figure 5C), thus significantly enhancing the metabolic activity (Figure 5D). We did not detect significant differences in glucose consumption or metabolic rates when DCs were stimulated with PM in the presence of alum (Figure 5C,D), suggesting that alum did not alter glucose uptake but its final metabolic fate. To test whether PM alone or in combination with alum affect mitochondrial activity in hmoDCs, we monitored changes in mitochondrial membrane potential (Δψ) with MitoTracker Red CMXRos. The mitochondrial Δψ was significantly increased by PM plus alum (Figure 5E), suggesting that alum has influence on the glucose metabolic fate by favouring mitochondrial oxidative phosphorylation. Further analysis of the

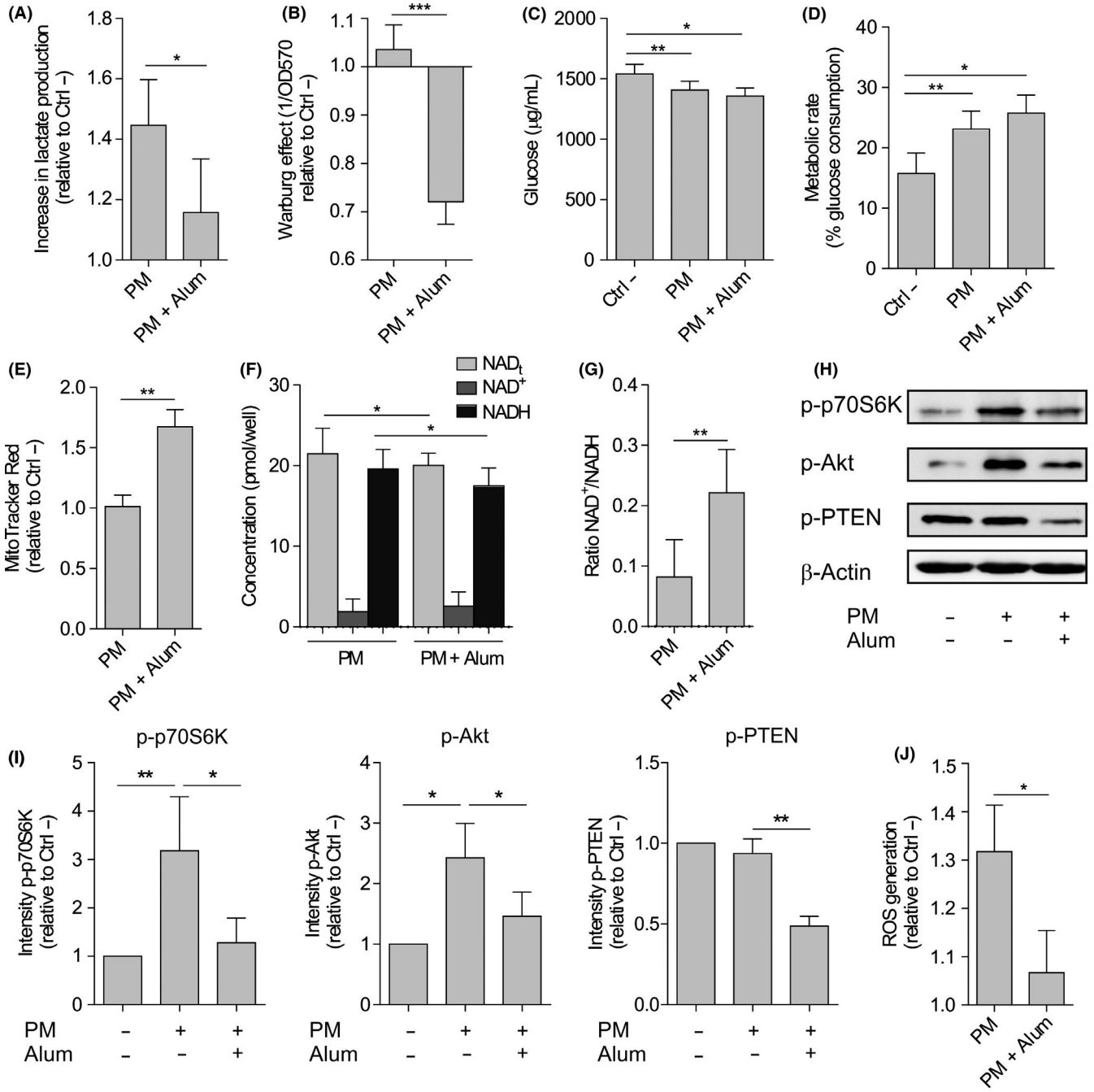

FIGURE 5 Alum alters the metabolic reprogramming induced by PM in human DCs from healthy donors. A, Lactate content in cell-free supernatants from PM- or PM and alum-stimulated hmoDCs after 18 h relative to the unstimulated (Ctrl -) condition (n = 6). B, Quantification of the induced Warburg effect relative to the unstimulated (Ctrl -) condition (n = 6). C, Glucose consumption by stimulated DCs and (D) calculated metabolic rate (n = 6). E, Fluorescence intensity of stimulated hmoDCs stained with MitoTracker Red (n = 5). F, Cellular redox status analysed based on the determination of NAD$^+$, NADH and total NAD levels (NADt) (n = 5). G, NAD$^+$/NADH ratios. H, Western blot analysis of protein extracts from hmoDCs stimulated for 30 min in the indicated conditions, and one representative example out of 4 is shown. I, Quantification of the reactive phosphorylated bands by scanning densitometry (mean ± SEM of n = 4 independent experiments). J, Intracellular ROS quantification in hmoDCs after 18 h of stimulation with PM or PM and alum (n = 6). Paired Student *t* test: **P* < .05, ***P* < .01 and ****P* < .001

redox status showed that the NADH accumulation induced by PM in hmoDCs was significantly reduced in the presence of alum (Figure 5F). Consequently, the NAD$^+$/NADH ratio was significantly higher in hmoDCs stimulated with PM plus alum than with PM alone (Figure 5G). Next, we studied the potential implication of mTOR pathway in the observed effects as a key regulator of metabolic responses. PM induced the rapid activation of mTOR pathway in hmoDCs as determined by the phosphorylation of its downstream substrate p70S6 kinase (Thr389) and its upstream activator Akt (Ser473) (Figure 5H,I). The phosphorylation of both

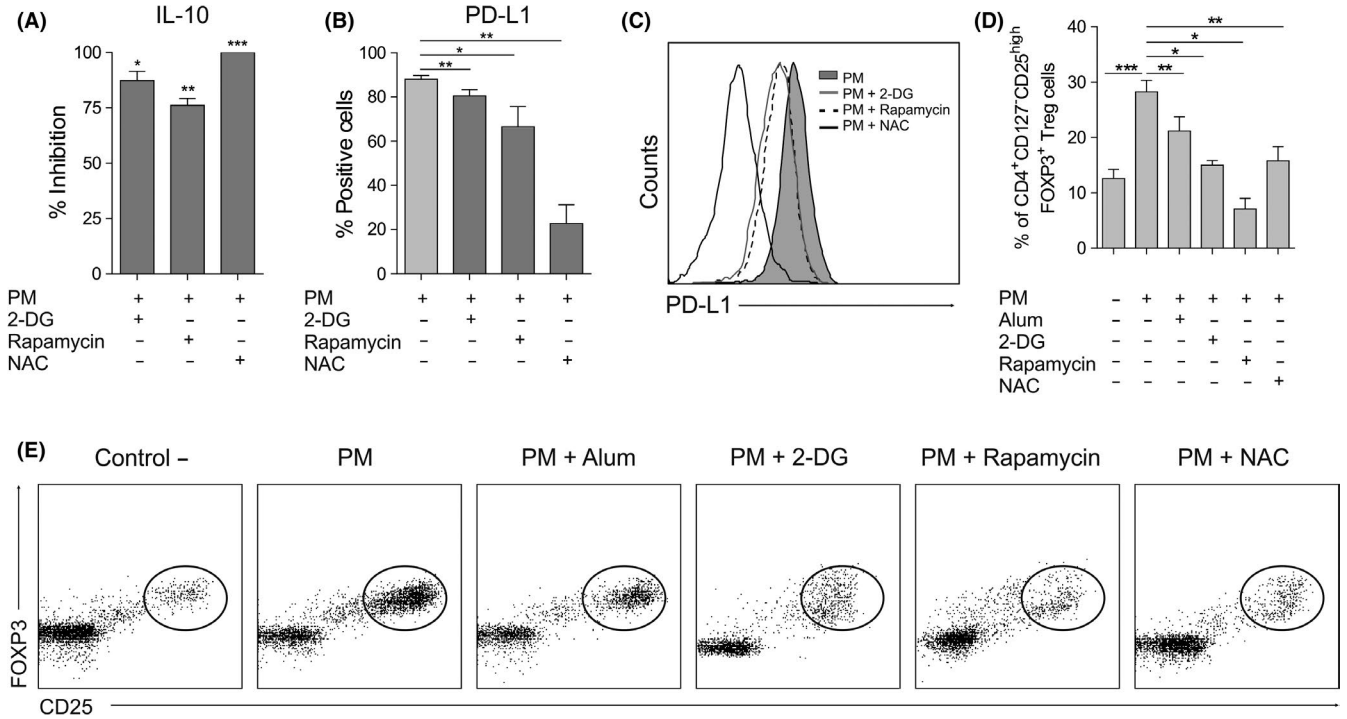

FIGURE 6 Influence of mTOR pathway, glycolysis and ROS production in the induction of human tolerogenic DCs by PM. A-C, IL-10 production (n = 6; A), percentage of hmoDCs expressing PD-L1 (n = 6; B) and flow cytometry representative histogram of PD-L1 expression (C) of hmoDCs after stimulation with PM for 18 h in the presence of 2-DG, NAC or rapamycin. D, $CD4^{+}CD25^{high}CD127^{-}FOXP3^{+}$ Treg cells generated after 5 d by allogeneic hmoDCs stimulated in the indicated conditions (gating in lymphocytes, n = 5). E, Flow cytometry representative dot plots of the generated $CD4^{+}CD25^{high}CD127^{-}FOXP3^{+}$ Treg cells under the indicated conditions. Paired Student *t* test: $^{*}P < .05$, $^{**}P < .01$ and $^{***}P < .001$

p70S6 kinase and Akt was inhibited when hmoDCs were activated by PM plus alum (Figure 5H,I), indicating that alum inhibits the PM-induced activation of mTOR. Supporting these data, alum also inhibited the phosphorylation of phosphate and tensin homologue (PTEN) (Ser380/Thr382/383), an inhibitor of mTOR signalling pathway that remains inactive while it is phosphorylated (Figure 5H,I). In addition to its role in glycolytic metabolism, previous studies showed a positive interplay between PI3K/Akt/mTOR signalling pathway and the regulation of ROS production.[25] PM treatment significantly increased ROS production in hmoDCs, which was significantly inhibited in the presence of alum (Figure 5J). Collectively, our results demonstrate that alum impairs the PM-induced activation of mTOR and metabolic reprogramming in hmoDCs.

3.6 | Glycolytic metabolism, mTOR activation and ROS production contribute to the tolerogenic properties imprinted by PM in hmoDCs that are impaired by alum

The inhibition of glycolysis with 2-DG, mTOR with rapamycin and ROS activity with NAC in PM-activated hmoDCs significantly suppressed the production of the anti-inflammatory cytokine IL-10 (Figure 6A). Similarly, the inhibition of glycolysis, mTOR and ROS activity significantly decreased the expression of PD-L1 in PM-activated hmoDCs (Figure 6B). Representative histograms of PD-L1 expression in PM-activated hmoDCs under the different conditions are displayed (Figure 6C). To assess the relevance of these findings in the generation of $FOXP3^{+}$ Treg cells by PM, we performed coculture experiments with PM-activated hmoDCs in the presence of the different inhibitors. As expected by the previous experiments, alum significantly reduced the frequency of PM-induced $FOXP3^{+}$ Treg cells (Figure 6D). Similarly, inhibition of glycolysis with 2-DG, mTOR with rapamycin and ROS activity with NAC in PM-activated hmoDCs significantly reduced the percentage of induced $FOXP3^{+}$ Treg cells (Figure 6D,E). These data suggest that (i) these pathways contribute to the induction of $FOXP3^{+}$ Treg cells by PM-activated DCs and (ii) alum impairs such induction through its inhibitory effect on these signalling pathways.

4 | DISCUSSION

In this study, we show that alum impairs the tolerogenic properties imprinted by allergoids conjugated to nonoxidized mannan. Alum decreases the expression of PD-L1 and IL-10 production in PM-activated human DCs, reducing their capacity to generate functional $FOXP3^{+}$ Treg cells. Mechanistically, we demonstrated that alum inhibits mTOR activation, shifts glycolysis metabolism and reduces

ROS production in human PM-activated DCs, thus impairing the tolerogenic properties promoted by PM. Subcutaneous immunizations of mice with PM adsorbed to alum induces a shift to allergic responses and impairs the induction of splenic FOXP3$^+$ Treg cells supporting the in vitro results with human cells. Remarkably, alum did not alter the capacity of PM to produce IgG-blocking antibodies with similar functional activity than those generated by PM in the absence of alum. Overall, our data point against the use of alum in order to preserve the tolerogenic properties imprinted by allergoids conjugated to mannan in DCs. This should be also taken into account when considering novel vaccination approaches aimed to induce tolerogenic DCs,[26,27] especially when the mTOR pathway is involved in such effects.[28] This might be also relevance for those vaccines based on triggering trained immunity, in which the Akt/mTOR activation is essential.[29,30]

This is a paradigmatic study revealing the importance of the better understanding of the molecular mechanisms driving alum adjuvanticity in the context of allergy, especially in humans, to continue improving allergen vaccine formulations for AIT. Allergoid-mannan conjugates represent a major development in the search of novel vaccine approaches to improve AIT,[6,9-11] and Alum was introduced as a vaccine adjuvant in 1926 by Glenny et al,[31] and since 1937, it is used in AIT. Although there are different adjuvant preparations that can be used in AIT as immunostimulants (ie, mineral salts or TLR-targeting adjuvants) or delivery systems (ie, different types of micro- and nanoparticles),[11] nowadays most of the subcutaneous vaccines for AIT include alum as adjuvant.[15] Although it is considered safe in terms of acute local or systemic effects,[18] the molecular mechanisms driving alum adjuvanticity are not completely understood.[20] Alum polarizes responses into Th2 cells in mice, whereas in humans there is still controversy.[32-34] Recent findings showed that alum can also activate innate immune responses in DCs and macrophages.[19,20] Here, we performed a comprehensive immunologic study of the potential influence of alum in the tolerogenic effects imprinted by PM targeting CLRs in DCs.[9] Alum significantly decreases the production of IL-10 and PD-L1 expression in human PM-activated DCs, which are molecules involved in the generation of functional Treg cells.[35,36] In contrast, the OX40-L expression, a molecule favouring Th2 polarization,[37,38] is significantly increased in the presence of alum. At the T-cell level, we showed that in humans, alum (in the presence of PM) not only promotes Th2 responses but also a broad pro-inflammatory profile, with Th1 and Th17 cells being also enhanced, whereas inhibiting the generation of functional FOXP3$^+$ Treg cells. Up to now, no data showing cross-talk between CLR- and alum-mediated signalling pathways have been reported. Alum is sensed by membrane lipids on DCs inducing activation in a receptor-independent manner that is mediated by the Syk-PI3K pathway.[20,39] PM trigger CLRs such as Syk-coupled Dectin-2 or DC-SIGN, both involved in PD-L1 expression and cytokine signature in human PM-activated DCs.[9] Our data clearly suggest that alum interferes with the CLR-mediated signalling pathways activated by PM in DCs.

Metabolic reprogramming plays a very important role in the control of DCs' function by regulating tolerogenicity *vs.* immunogenicity.[21,22] mTOR is a central regulator of cell metabolism, growth, proliferation and survival.[40,41] To gain insight into potential novel molecular mechanisms involved in the observed effects, we studied metabolic changes induced by PM in DCs and how alum could interfere on them. PM rapidly activates mTOR signalling pathway and PM-activated DCs display a high rate of glycolysis and lactic acid fermentation (Warburg effect),[40,42] features that were impaired by alum. Increased mTOR pathway activity is correlated with enhanced glycolysis, which appears to be associated with the generation of peripherally induced Treg cells.[21] Lactate has been also shown to enhance IL-10 production in macrophages and DCs.[43] It is well-recognized that TLR activation in DCs and macrophages induces a glycolytic burst,[44,45] but data for CLRs are mostly limited to Dectin-1 activated by β-glucan.[29] We demonstrate that mTOR activation is implicated in the induction of IL-10 and PD-L1 in human PM-activated DCs. Schülke *et al* also described that in mDCs activated by the fusion protein rFlaA:Betv1, mTOR regulates IL-10 production.[28] Similarly, the expression of PD-L1, a key molecule for the induction of functional FOXP3$^+$ Treg cells,[36,46,47] has been shown to be regulated by mTOR in DCs.[48] Herein, we show that the inhibition of PM-induced mTOR signalling and the reduction in PD-L1 expression in DCs by alum correlate with a reduction on the generation of FOXP3$^+$ Treg cells. Supporting this view, SH2 domain-containing inositol 5'-phosphatase (SHIP)-deficient mice, in which the Akt/mTOR pathway is upregulated on myeloid cells,[49] show a remarkable increase in FOXP3$^+$ Treg cells.[50]

Tolerogenic DCs display enhanced glycolytic capacity and ROS production with respect to mature pro-inflammatory DCs.[51] PM significantly increases intracellular ROS in human DCs, which were inhibited by alum. Recently, D-mannose treatment increased ROS production in T cells compared with TCR stimulation alone.[52] In line with our results, blockade of ROS activity by NAC significantly reduced numbers of D-mannose-induced Treg cells.[52] Although ROS have been considered toxic products of cellular metabolism, increasing evidence supports the idea that low amounts of ROS are positive contributors to normal signalling pathways.[42,53] Previous studies demonstrated that ROS further activates Akt/mTOR pathway, enabling optimal T-cell proliferation and glycolysis.[53-55] Therefore, our results confirm that the inhibition of ROS production and the blockade of mTOR signalling by alum in PM-activated DCs represent novel mechanisms by which this adjuvant impairs the induction of Treg cells.

Interestingly, mice immunized with PM in the presence of alum display significantly lower numbers of splenic FOXP3$^+$ Treg cells and higher IFN-γ, IL-5 and IL-4 levels than mice immunized only with PM. The ratio of serum IgG1/IgG2a is significantly higher in mice immunized with PM plus alum, indicating that alum also impairs in vivo tolerogenic responses to PM. Remarkably, alum did not enhance the capacity of PM to induce allergen-specific antibodies with blocking activity, indicating that the absence of alum in PM vaccine formulations would not significantly modify this feature.

In conclusion, this study provides novel insights into molecular pathways that might be affected by alum as adjuvant in AIT. We uncover novel molecular mechanisms involving mTOR, glycolysis and ROS production by which alum interferes with CLR-mediated signalling pathways activated by polymerized allergoids conjugated

to nonoxidized mannan in human DCs, thus impairing the imprinted tolerogenic properties. This study demonstrates the importance of understanding the influence of adjuvants such as alum in novel vaccine formulations for AIT. Future studies on how other approved adjuvants for AIT might influence the tolerogenic features imprinted by allergoids conjugated to mannan could also contribute to provide novel mechanistic insights into their way of action. Finally, our findings might well go beyond AIT formulations and could be also relevant for other types of vaccines such as those promoting innate trained immunity, in which mTOR activation and metabolic reprogramming represent key mechanistic events in their mode of action.

ACKNOWLEDGEMENTS

This work was supported by grants SAF-2017-84978-R to OP from MINECO, Spain, and by grants IDI-20110410 and IDI-20141131 to Inmunotek SL from CDTI and MINECO. CB-V. and MP are recipients of FPU and FPI fellowships, respectively, from MINECO. IS is recipient of Torres Quevedo grant (PTQ-12-05785), from MINECO, Spain.

CONFLICTS OF INTEREST

OP has received payment for lectures and participation in Advisory Boards from Allergy Therapeutics, Amgen, AstraZeneca, Inmunotek SL, Novartis, Sanofi Genzyme and Stallergenes. OP has received research grants from Inmunotek SL and Novartis SL. JLS is the founder and CEO of Inmunotek SL. EF-C. is a shareholder and employee of Inmunotek SL. IS is an employee of Inmunotek. The rest of the authors declare no competing financial interests.

AUTHOR CONTRIBUTIONS

OP and JLS conceived and designed the study. C. B.-V. (human experiments), IS (mice experiments) and M. P.-D. (technical support for human experiments) performed the experiments. E. F.-C, JLS and O.P provided reagents. C. B.-V., IS, M. P.-D., EF-C., JLS and O.P analysed and discussed the data. OP and C. B.-V wrote the paper. All the authors read and approved the final version of the manuscript.

ORCID

Cristina Benito-Villalvilla https://orcid.org/0000-0002-5544-0199
Enrique Fernández-Caldas https://orcid.org/0000-0001-5873-6932
José Luis Subiza https://orcid.org/0000-0002-0134-5321
Oscar Palomares https://orcid.org/0000-0003-4516-0369

REFERENCES

1. Mahler V, Esch RE, Kleine-Tebbe J, et al. Understanding differences in allergen immunotherapy products and practices in North America and Europe. *J Allergy Clin Immunol.* 2019;143(3):813-828.
2. Dhami S, Nurmatov U, Arasi S, et al. Allergen immunotherapy for allergic rhinoconjunctivitis: a systematic review and meta-analysis. *Allergy.* 2017;72(11):1597-1631.
3. Jutel M, Agache I, Bonini S, et al. International consensus on allergen immunotherapy II: mechanisms, standardization, and pharmacoeconomics. *J Allergy Clin Immunol.* 2016;137(2):358-368.
4. Shamji MH, Durham SR. Mechanisms of allergen immunotherapy for inhaled allergens and predictive biomarkers. *J Allergy Clin Immunol.* 2017;140(6):1485-1498.
5. Palomares O, Akdis M, Martin-Fontecha M, Akdis CA. Mechanisms of immune regulation in allergic diseases: the role of regulatory T and B cells. *Immunol Rev.* 2017;278(1):219-236.
6. Berings M, Karaaslan C, Altunbulakli C, et al. Advances and highlights in allergen immunotherapy: on the way to sustained clinical and immunologic tolerance. *J Allergy Clin Immunol.* 2017;140(5):1250-1267.
7. Bousquet J, Pfaar O, Togias A, et al. ARIA care pathways for allergen immunotherapy. *Allergy.* 2019;2019. https://doi.org/10.1111/all.13805. [Epub ahead of print]
8. Pfaar O, Lou H, Zhang Y, Klimek L, Zhang L. Recent developments and highlights in allergen immunotherapy. *Allergy.* 2018;73(12):2274-2289.
9. Sirvent S, Soria I, Cirauqui C, et al. Novel vaccines targeting dendritic cells by coupling allergoids to nonoxidized mannan enhance allergen uptake and induce functional regulatory T cells through programmed death ligand 1. *J Allergy Clin Immunol.* 2016;138(2):558.
10. Schulke S, Vieths S. Dendritic cell targeting with C-type lectins for improvement of allergen immunotherapy. *J Allergy Clin Immunol.* 2016;138(2):568-570.
11. Benito-Villalvilla C, Soria I, Subiza JL, Palomares O. Novel vaccines targeting dendritic cells by coupling allergoids to mannan. *Allergo J Int.* 2018;27:256-262.
12. Manzano AI, Canada FJ, Cases B, et al. Structural studies of novel glycoconjugates from polymerized allergens (allergoids) and mannans as allergy vaccines. *Glycoconj J.* 2016;33(1):93-101.
13. Soria I, Lopez-Relano J, Vinuela M, et al. Oral myeloid cells uptake allergoids coupled to mannan driving Th1/Treg responses upon sublingual delivery in mice. *Allergy.* 2018;73:875-884.
14. Soria I, Alvarez J, Manzano AI, et al. Mite allergoids coupled to nonoxidized mannan from Saccharomyces cerevisae efficiently target canine dendritic cells for novel allergy immunotherapy in veterinary medicine. *Vet Immunol Immunopathol.* 2017;190:65-72.
15. Klimek L, Schmidt-Weber CB, Kramer MF, Skinner MA, Heath MD. Clinical use of adjuvants in allergen-immunotherapy. *Expert Rev Clin Immunol.* 2017;13(6):599-610.
16. Moingeon P. Adjuvants for allergy vaccines. *Hum Vaccin Immunother.* 2012;8(10):1492-1498.
17. Pfaar O, Bonini S, Cardona V, et al. Perspectives in allergen immunotherapy: 2017 and beyond. *Allergy.* 2018;73(suppl 104):5-23.
18. Jensen-Jarolim E. Aluminium in allergies and allergen immunotherapy. *World Allergy Organ J.* 2015;8(1):7.
19. Kool M, Fierens K, Lambrecht BN. Alum adjuvant: some of the tricks of the oldest adjuvant. *J Med Microbiol.* 2012;61(Pt 7):927-934.
20. Oleszycka E, Lavelle EC. Immunomodulatory properties of the vaccine adjuvant alum. *Curr Opin Immunol.* 2014;28:1-5.
21. O'Neill LA, Kishton RJ, Rathmell J. A guide to immunometabolism for immunologists. *Nat Rev Immunol.* 2016;16(9):553-565.
22. O'Neill LA, Pearce EJ. Immunometabolism governs dendritic cell and macrophage function. *J Exp Med.* 2016;213(1):15-23.
23. Lechmann M, Berchtold S, Hauber J, Steinkasserer A. CD83 on dendritic cells: more than just a marker for maturation. *Trends Immunol.* 2002;23(6):273-275.
24. Ito T, Wang YH, Duramad O, et al. TSLP-activated dendritic cells induce an inflammatory T helper type 2 cell response through OX40 ligand. *J Exp Med.* 2005;202(9):1213-1223.

25. Silva A, Girio A, Cebola I, Santos CI, Antunes F, Barata JT. Intracellular reactive oxygen species are essential for PI3K/Akt/mTOR-dependent IL-7-mediated viability of T-cell acute lymphoblastic leukemia cells. *Leukemia.* 2011;25(6):960-967.
26. Florez-Grau G, Zubizarreta I, Cabezon R, Villoslada P, Benitez-Ribas D. Tolerogenic dendritic cells as a promising antigen-specific therapy in the treatment of multiple sclerosis and neuromyelitis optica from preclinical to clinical trials. *Front Immunol.* 2018;9:1169.
27. Yoo S, Ha SJ. Generation of tolerogenic dendritic cells and their therapeutic applications. *Immune Netw.* 2016;16(1):52-60.
28. Schulke S, Fiedler AH, Junker AC, et al. Critical role of mammalian target of rapamycin for IL-10 dendritic cell induction by a flagellin A conjugate in preventing allergic sensitization. *J Allergy Clin Immunol.* 2018;141(5):1786.
29. Mulder W, Ochando J, Joosten L, Fayad ZA, Netea MG. Therapeutic targeting of trained immunity. *Nat Rev Drug Discov.* 2019;18(7):553-566.
30. Sanchez-Ramon S, Conejero L, Netea MG, Sancho D, Palomares O, Subiza JL. Trained immunity-based vaccines: a new paradigm for the development of broad-spectrum anti-infectious formulations. *Front Immunol.* 2018;9:2936.
31. Glenny AT, Pope CG, Waddington H, Wallace U. Immunological notes XVLL.-XXIV. *J Pathol Bacteriol.* 1926;29(1):31-40.
32. Brunner R, Wallmann J, Szalai K, et al. Aluminium per se and in the anti-acid drug sucralfate promotes sensitization via the oral route. *Allergy.* 2009;64(6):890-897.
33. Marichal T, Ohata K, Bedoret D, et al. DNA released from dying host cells mediates aluminum adjuvant activity. *Nat Med.* 2011;17(8):996-1002.
34. Hogenesch H. Mechanism of immunopotentiation and safety of aluminum adjuvants. *Front Immunol.* 2012;3:406.
35. Rabe H, Nordstrom I, Andersson K, Lundell AC, Rudin A. Staphylococcus aureus convert neonatal conventional CD4(+) T cells into FOXP3(+) CD25(+) CD127(low) T cells via the PD-1/PD-L1 axis. *Immunology.* 2014;141(3):467-481.
36. Gollwitzer ES, Saglani S, Trompette A, et al. Lung microbiota promotes tolerance to allergens in neonates via PD-L1. *Nat Med.* 2014;20(6):642-647.
37. Jenkins SJ, Perona-Wright G, Worsley AG, Ishii N, MacDonald AS. Dendritic cell expression of OX40 ligand acts as a costimulatory, not polarizing, signal for optimal Th2 priming and memory induction in vivo. *J Immunol.* 2007;179(6):3515-3523.
38. Gori S, Vermeulen M, Remes-Lenicov F, et al. Acetylcholine polarizes dendritic cells toward a Th2-promoting profile. *Allergy.* 2017;72(2):221-231.
39. Flach TL, Ng G, Hari A, et al. Alum interaction with dendritic cell membrane lipids is essential for its adjuvanticity. *Nat Med.* 2011;17(4):479-487.
40. Linke M, Fritsch SD, Sukhbaatar N, Hengstschlager M, Weichhart T. mTORC1 and mTORC2 as regulators of cell metabolism in immunity. *FEBS Lett.* 2017;591(19):3089-3103.
41. Zeng H, Chi H. mTOR signaling in the differentiation and function of regulatory and effector T cells. *Curr Opin Immunol.* 2017;46:103-111.
42. Franchina DG, Dostert C, Brenner D. Reactive oxygen species: involvement in T cell signaling and metabolism. *Trends Immunol.* 2018;39(6):489-502.
43. Weichhart T, Hengstschlager M, Linke M. Regulation of innate immune cell function by mTOR. *Nat Rev Immunol.* 2015;15(10):599-614.
44. Perrin-Cocon L, Aublin-Gex A, Diaz O, et al. Toll-like receptor 4-induced glycolytic burst in human monocyte-derived dendritic cells results from p38-dependent stabilization of HIF-1alpha and increased hexokinase II expression. *J Immunol.* 2018;201(5):1510-1521.
45. Pearce EJ, Everts B. Dendritic cell metabolism. *Nat Rev Immunol.* 2015;15(1):18-29.
46. de Roock S, Hoeks SB, Meurs L, et al. Critical role for programmed death 1 signaling and protein kinase B in augmented regulatory T-cell induction in cord blood. *J Allergy Clin Immunol.* 2011;128(6):1369-1371.
47. Francisco LM, Salinas VH, Brown KE, et al. PD-L1 regulates the development, maintenance, and function of induced regulatory T cells. *J Exp Med.* 2009;206(13):3015-3029.
48. Sukhbaatar N, Hengstschlager M, Weichhart T. mTOR-mediated regulation of dendritic cell differentiation and function. *Trends Immunol.* 2016;37(11):778-789.
49. Saz-Leal P, Del Fresno C, Brandi P, et al. Targeting SHIP-1 in myeloid cells enhances trained immunity and boosts response to infection. *Cell Rep.* 2018;25(5):1118-1126.
50. Collazo MM, Wood D, Paraiso KH, et al. SHIP limits immunoregulatory capacity in the T-cell compartment. *Blood.* 2009;113(13):2934-2944.
51. Malinarich F, Duan K, Hamid RA, et al. High mitochondrial respiration and glycolytic capacity represent a metabolic phenotype of human tolerogenic dendritic cells. *J Immunol.* 2015;194(11):5174-5186.
52. Zhang D, Chia C, Jiao X, et al. D-mannose induces regulatory T cells and suppresses immunopathology. *Nat Med.* 2017;23(9):1036-1045.
53. Yalcin S, Marinkovic D, Mungamuri SK, et al. ROS-mediated amplification of AKT/mTOR signalling pathway leads to myeloproliferative syndrome in Foxo3(-/-) mice. *EMBO J.* 2010;29(24):4118-4131.
54. Barnes PJ. Mechanisms of development of multimorbidity in the elderly. *Eur Respir J.* 2015;45(3):790-806.
55. Previte DM, O'Connor EC, Novak EA, Martins CP, Mollen KP, Piganelli JD. Reactive oxygen species are required for driving efficient and sustained aerobic glycolysis during CD4+ T cell activation. *PLoS One.* 2017;12(4):e0175549.

SUPPORTING INFORMATION

Additional supporting information may be found online in the Supporting Information section at the end of the article.

How to cite this article: Benito-Villalvilla C, Soria I, Pérez-Diego M, Fernández-Caldas E, Subiza JL, Palomares O. Alum impairs tolerogenic properties induced by allergoid-mannan conjugates inhibiting mTOR and metabolic reprogramming in human DCs. *Allergy.* 2020;75:648–659. https://doi.org/10.1111/all.14036

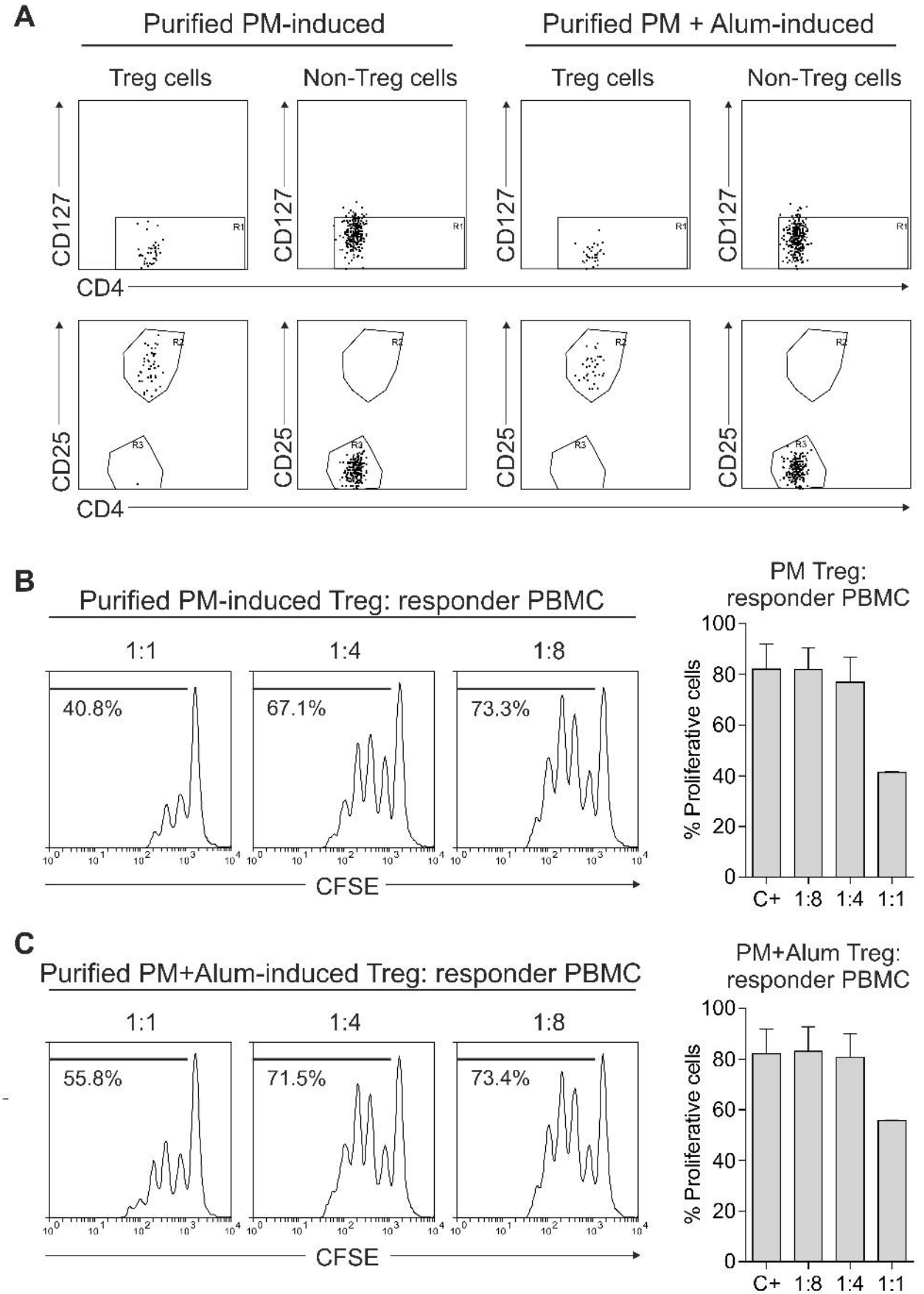

Figure supplementary 1. Benito-Villalvilla et al.

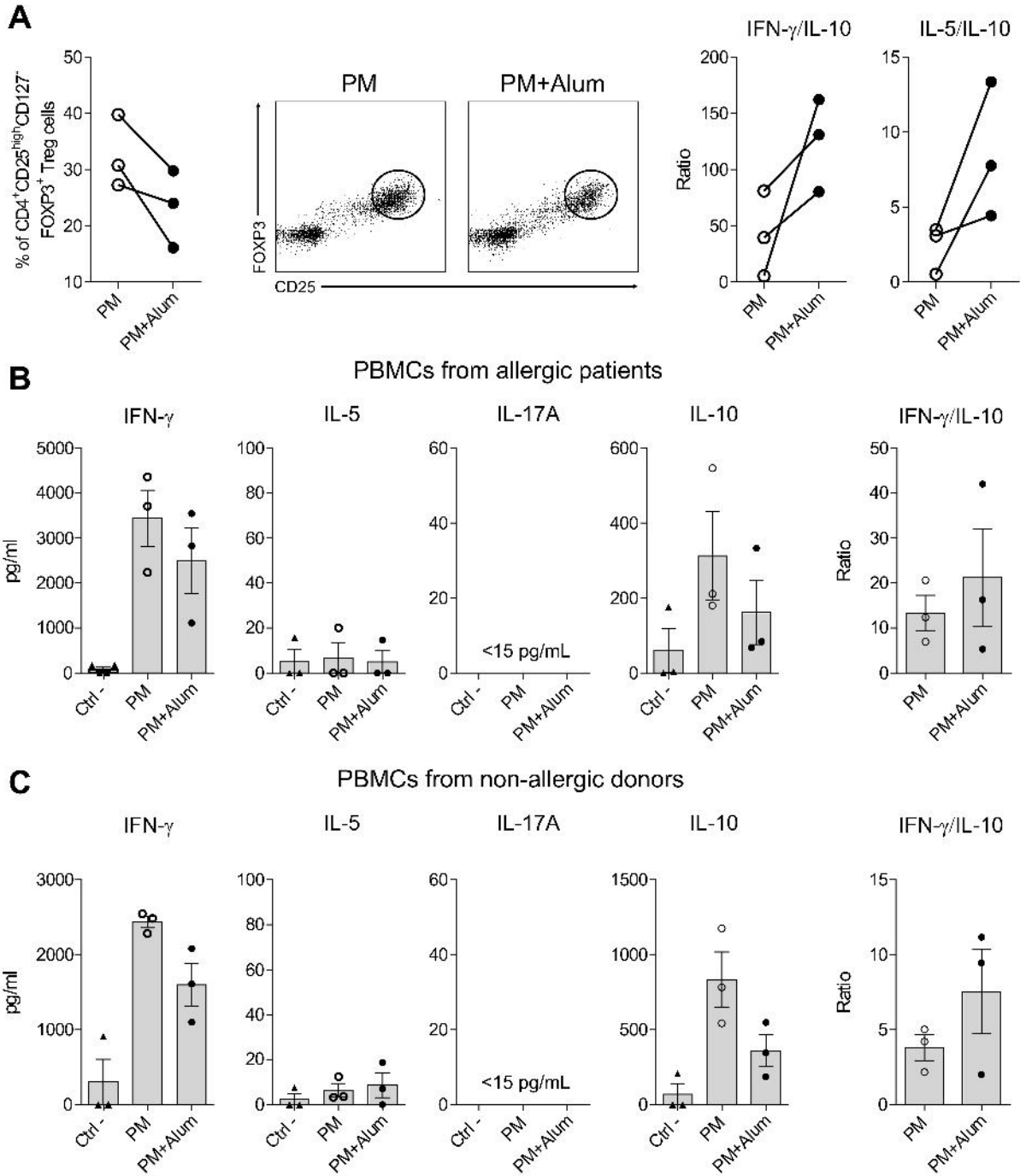

Figure supplementary 2. Benito-Villalvilla et al.

TITLE PAGE

Alum impairs tolerogenic properties induced by allergoid-mannan conjugates inhibiting mTOR and metabolic reprogramming in human DCs

RUNNING TITLE: Alum breaks tolerance induced by allergoid-mannan conjugates

Cristina Benito-Villalvilla, BSc,[1], Irene Soria, PhD,[2], Mario Pérez-Diego, BSc,[1], Enrique Fernández-Caldas, PhD,[2,3], José Luis Subiza, MD, PhD,[2], Oscar Palomares, PhD[1]

[1] Department of Biochemistry and Molecular Biology, School of Chemistry, Complutense University, Madrid, Spain
[2] Inmunotek, Alcalá de Henares, Madrid, Spain
[3] University of South Florida, College of Medicine, Tampa, USA.

Corresponding Author: Oscar Palomares, PhD
Department of Biochemistry and Molecular Biology,
School of Chemistry, Complutense University of Madrid,
Avenida Complutense s/n,
28040 Madrid, Spain
Telephone: + 34 913944159
Email: oscar.palomares@quim.ucm.es

ACKNOLEDGEMENTS

This work was supported by grants SAF-2017-84978-R to O.P. from MINECO, Spain and by grants IDI-20110410 and IDI-20141131 to Inmunotek SL from CDTI and MINECO. C.B.-V. and M.P. are recipients of FPU and FPI fellowships, respectively, from MINECO. I.S. is recipient of Torres Quevedo grant (PTQ-12-05785), from MINECO, Spain.

CONFLICT OF INTERESTS

O.P. has received payment for lectures and participation in Advisory Boards from Allergy Therapeutics, Amgen, AstraZeneca, Inmunotek SL, Novartis, Sanofi-Genezyme and Stallergenes. OP has received research grants from Inmunotek SL and Novartis SL. J.L.S. is the founder and CEO of Inmunotek SL. E.F.-C. is a shareholder and employee of Inmunotek SL. I.S. is an employee of Inmunotek. The rest of authors declare no competing financial interests.

METHODS

HmoDCs generation, naive CD4$^+$ T cells purification and total blood DCs isolation

Peripheral blood mononuclear cells (PBMC) were obtained from buffy coats of healthy donors or allergic patients by Ficoll density gradient centrifugation (800g, 20 minutes). Immature hmoDCs were generated from blood monocytes obtained from total PBMCs using anti-CD14 microbeads and cultured for 6 days with RPMI medium containing 100 ng/mL of IL-4 and GM-CSF (PeproTeck, Rocky Hill, NJ). The purity and phenotype of monocytes and generated immature hmoDCs were analysed by flow cytometry with lineage-specific markers. Peripheral blood naive CD4$^+$ T cells were isolated using the ‘‘Naive CD4$^+$ T Cell Isolation Kit’’ (Miltenyi Biotec) and total dendritic cell fraction was obtained from PBMC with ‘‘Blood Dendritic Cell Isolation Kit II’’ (Miltenyi Biotec), according to manufacturer’s protocol.

PBMCs from healthy donors or allergic patients were stimulated with medium (Ctrl -), PM (50 µg/mL) or PM with alum (0.1 mg/mL) for 3 days. Cell-free supernatants were used to quantify IL-10, IL-5, IFN-γ and IL-17A by ELISA.

Flow cytometry

Cells were washed with PBS/EDTA 2 mM/0.5% BSA and stained for 15 minutes at room temperature in the darkness. The corresponding isotype controls were included in each staining (IgG2A-FITC, IgG1-PE, IgG2A-PerCP, or IgG1-APC). Flow cytometric monoclonal antibodies were purchased from Miltenyi Biotec (Bergisch Gladbach, Germany): human anti-HLA-DR-fluorescein isothiocyanate [FITC], anti–HLA-DR–allophycocyanin [APC], anti-CD83–APC, anti-CD303–phycoerythrin [PE], anti-CD1c–FITC, anti-CD127–PE, FcR Blocking; BioLegend (San Diego, CA): human anti-FOXP3–Alexa Fluor 488, anti-CD25–APC, anti-CD4–peridinin chlorophyll protein complex [PerCP], anti-IL-10-PE, anti-IL-17A-PE, anti-IL-5-PE, mouse anti-FOXP3–Alexa Fluor 488, mouse anti-CD4–PerCP, and mouse anti-CD25–PE; and BD PharMingen (San Jose, CA): human anti-PD-L1–FITC, anti-OX40L–PE, anti-CD3–

APC, anti-CD19–PE/Cy7, and anti-IFNγ–Alexa Fluor 488. For analysis of FOXP3 expression in human T cells primed with DCs, cells were first subjected to surface staining with anti-human CD4-PerCP, CD127-PE, and CD25-APC antibodies. After fixation and permeabilization, cells were stained with anti-human FOXP3-Alexa Fluor 488, according to manufacturer's recommendations. The same protocol described above was carried out for the phenotypic characterization of $CD4^{+}CD25^{high}FOXP3^{+}$ Treg cells in freshly isolated mouse splenocytes using anti-mouse CD4-PerCP and CD25-PE antibodies for surface staining and anti-mouse FOXP3-Alexa 488 for intranuclear staining. The corresponding isotype controls were included in each staining. Flow cytometry analysis was performed in a FACSCalibur cytometer (Beckton Dickinson) in the Cytometry and Fluorescence Microscopy Unit at Complutense University of Madrid.

Cytokine quantification

Concentrations of IL-6, IL-12p70, IL-4, IL-10, IFN-γ, and IL-5 in cell-free supernatants were quantified by sandwich ELISA using specific ELISA cytokine kits for each one (BD Biosciences, San Jose, CA). IL-23 and IL-17A levels were quantified by Human IL-23 ELISA Ready-SET-Go! (e-Biosciences, San Diego, CA) and quantikine Elisa Kit (RD Systems), respectively. In all cases, manufacturer's instructions were followed with minor modifications.

Coculture experiments

HmoDCs or human total blood DC enriched fraction treated with medium (Ctrl -), alum (0.1 mg/mL), PM (50 µg/mL) or the combination of PM and alum were cocultured with purified allogeneic naïve $CD4^{+}$ T cells (DC/T cell ratio of 1:5) for 5 days. IL-17A, IFN-γ, IL-5 and IL-10 were quantified in cell-free supernatants by ELISA. For intracellular cytokine production, the primed $CD4^{+}$ T cells were washed and restimulated with 25 ng/mL PMA plus 1 mg/mL ionomycin for 6 hours. 10 µg/mL brefeldin A was added during the last 4 hours. Cells were fixed and permeabilized with Cytofix/Cytoperm (BD

Biosciences) according to the manufacturer's instructions. Cells were stained with fluorochrome-labeled mAbs to IL-17A, IFN-γ, IL-5, and IL-10.

Treg cell suppression assay

$CD4^{+}CD25^{high}CD127^{-}FOXP3^{+}$ Treg cells induced by allogeneic PM- or PM in the presence of alum-stimulated hmoDCs were purified by cell sorting of $CD4^{+}CD25^{high}CD127^{-}$ population and mixed with CFSE-labeled autologous PBMCs (responder cells) at different ratios and stimulated with plate-bound anti-human CD3 antibody (1 mg/mL, clone OKT3; eBioscience) and soluble anti-human CD28 (1 mg/mL, clone CD28.6; eBioscience) for 5 days. For control purposes, CFSE-labeled PBMCs were cultured alone with or without stimulation, and non-Treg cells (negative fraction of the sorting) were also tested. Proliferation of $CD4^{+}$ T cells was determined by using CFSE dilution with flow cytometry.

Metabolic studies

The Warburg effect in stimulated hmoDC cultures was determined photometrically 18 hours after stimulation by quantifying the OD at 570 nm and calculating the Warburg effect as 1/OD570 normalized to the unstimulated. Glucose concentrations in culture supernatants were determined 18 hours after stimulation by using the Glucose (GO) Assay Kit (Sigma-Aldrich). The metabolic rate was derived mathematically in percentage of medium without DCs (glucose concentration in RPMI 1640 = 2 mg/mL). Lactate concentrations in culture supernatants were determined 18 hours after stimulation by using the colorimetric L-Lactate Assay kit (Abcam), according to the manufacturer's recommendations. To measure mitochondrial membrane potential, MitoTracker Red CMXRos was used (250 nM, Thermo Fisher Scientific). Total NAD^{+}/nicotinamide adenine dinucleotide (NADH) content, NAD^{+}, and NADH concentrations in lysates of DCs were determined by using NAD/NADH Assay Kit (Abcam), according to the manufacters' recommendations. Reactive oxygen species were measured by DCFDA Cellular ROS Detection Assay Kit (Abcam, Cambridge, United Kingdom) following manufacturer's instructions. Briefly, total ROS levels were

measured using the cell permeant reagent 2',7' –dichlorofluorescin diacetate (DCFDA). Cells were stained with DCDFA for 30 minutes at 37°C after 18 hours of treatment with the corresponding stimuli. Fluorescence was measured in a FLUOstar Omega microplate reader (Ex/Em = 485/535 nm).

Western blotting

Freshly isolated hmoDCs were treated with medium (Ctrl -), PM (50 µg/mL) and PM previously adsorbed to alum (0.1 mg/mL). After 30 minutes at 37°C, cells were harvested and lysed with RIPA buffer (ThermoFisher scientific, Madrid, Spain) supplemented with Protease/Phosphatase Inhibitor Cocktail (Cell Signaling, Danvers, Mass) for 30 minutes at 4°C with vortexing every 10 minutes. Lysates were centrifuged for 15 minutes at 10,000g and 4°C, and supernatants were collected for protein quantification with Micro BCA Kit (Pierce, Rockford, Ill). Ten micrograms of total protein from cell lysates was separated by means of SDS-PAGE and transferred onto a nitrocellulose membrane (Bio-Rad Laboratories, Hercules, Calif). The membrane was incubated with the indicated antibodies used as follows: phospho-PTEN (Ser380/Thr382/383) (1:1000, Cell Signaling), phospho-p70 S6 Kinase (Thr389) (1:500; Cell Signaling), phospho-Akt (Ser473) (1:1000; Cell Signaling) and β-actin (1:15000, Sigma) as primary antibodies and goat anti-rabbit (1/3000; Bio-Rad Laboratories) or goat anti-mouse (1:2500, Pierce) conjugated with horseradish peroxidase as a secondary antibody. Reactive bands were visualized with the ECL chemiluminescence system (Bio-Rad Laboratories). The OD of the reactive bands was quantified with Fujifilm multigauge software, and values were expressed relative to the β-actin loading control.

Immunization of mice with control, alum, PM, or PM with alum: quantification of induced serum allergen-specific immunoglobulins levels; and cytokine profiles of splenocytes stimulated in vitro with N

BALB/c female mice (6 weeks old) were immunized 3 times with 20 µg (200 µL at 100 µg/mL) of PM, or PM previously adsorbed to 2 mg of alum by means of subcutaneous injection every 15 days and killed 7 days after the last immunization. Serum specific IgG2a, IgG1, IgE reactivities to N induced with each treatment were determined by means of ELISA. Spleens were used to prepare single-cell suspensions according to conventional protocols. The presence of splenic $CD4^{+}CD25^{high}FOXP3^{+}$ Treg cells in the different immunized mice was quantified, as described above. Splenocytes were stimulated *in vitro* with N, and cytokine (IFN-γ, IL-5, IL-4 and IL-10) production was measured by using CBA Cytometric kits (Beckton Dickinson) in 48-hour culture supernatants. Animal experiments were approved by the Ethics Committee of Hospital Clínico San Carlos.

ELISA inhibition of the binding of serum IgE from allergic patients to N extract by blocking antibodies induced after immunization of mice.

The blocking capacity of the serum antibodies generated by means of immunization of mice with control, alum, PM, and PM with alum was analyzed by using ELISA inhibition assays. Microtiter plates (Corning Inc, Corning, NY) were coated with 10 µg of N in 100 µl of PBS overnight at 4°C. Plates were washed 3 times with PBS and 0.1% vol/vol Tween-20 and blocked for 1 hour with PBS, 0.1% vol/vol Tween-20, and 3% wt/vol dehydrated milk. Then plates were incubated with the serum of mice immunized against negative control, alum, PM, or PM with alum extracts. After 1 hour of incubation, plates were washed 4 times with PBS and 0.1% vol/vol Tween-20 and incubated for 2 hours with individual serum from 5 patients with well-defined grass pollen allergy diluted 1:50 in PBS, 0.1% vol/vol Tween-20, and 3% wt/vol dehydrated milk. The patients were previously described[1] and the study was approved by the Regional Ethics Committee of Comunidad Autónoma de Madrid (EudraCT: 2014-005471-88). After 4 washes, bound IgE antibodies were detected by incubating for 1 hour with biotin anti-human IgE rabbit monoclonal antibody (1:100000 diluted) (RevMab Biosciences, South San Francisco, CA), followed by 45 minutes with

horseradish peroxidase–coupled streptavidin (diluted 1:2500). The peroxidase reaction was developed by using fresh enzyme substrate (0.03% H_2O_2 and 0.63 mg/mL *o*-phenylenediamine in 0.1 mol/L sodium citrate, pH 5.0), and the reaction was stopped with 3 N H_2SO_4. OD was measured at 492 nm in an ELISA reader.

LEGEND TO SUPPLEMENTARY FIGURES

FIGURE S1. Suppression capacity of FOXP3$^+$ Treg cells induced by allogeneic PM or PM and alum-treated hmoDCs. (A) Representative dot plots of the purification of Treg cells by sorting. (B) and (C) Proliferation of CFSE-labeled PBMCs gated on CD4$^+$ cells after 5 days of coculture with autologous purified FOXP3$^+$ Treg cells induced by allogeneic PM-treated (Fig. S1B) or PM and alum-treated (Fig. S1C) hmoDCs. The percentages of proliferating responder PBMCs stimulated with anti-CD3 and anti-CD28 for each condition at different Treg cell/responder PBMC ratios are shown (n = 2).

FIGURE S2. Effects of alum in hmoDCs and PBMCs from allergic patients. (A) Percentage of induced CD4$^+$CD25^{high}CD127$^-$FOXP3$^+$ Treg cells and cytokine ratios produced by T cells primed by allogeneic PM or PM and alum-treated hmoDCs from allergic patients after 5 days (n = 3). (B) Cytokines and cytokine ratios produced by PBMCs from allergic patients stimulated with the indicated stimulus for 3 days (n = 3). (C) Cytokines and cytokine ratios produced by PBMCs from non-allergic donors stimulated with the indicated stimulus for 3 days (n = 3).

REFERENCES

1. Sirvent S, Soria I, Cirauqui C, et al. Novel vaccines targeting dendritic cells by coupling allergoids to nonoxidized mannan enhance allergen uptake and induce functional regulatory T cells through programmed death ligand 1. *J Allergy Clin Immunol.* 2016;138(2):558.